

# Practical Aspects of the Injection-Locked Hybrid Discriminator

TARAPRASAD CHATTOPADHYAY

**Abstract** — This paper analyzes the performance of an *X*-band (*I*-band) injection-locked hybrid discriminator taking into consideration such practical circuit effects as the presence of signal delay in different parts of the circuit, amplitude perturbation of the locked oscillator, and the reflection arising from a detector mismatch. Proposals are also made for the optimum design and the bandwidth extension of this tracking discriminator.

## I. INTRODUCTION

A NEW microwave-frequency discriminator utilizing a single magic tee and the technique of injection synchronization has recently been designed [1] and designated the injection-locked hybrid discriminator (ILHD). It has also been shown [1] that the bandwidth-sensitivity product of this ILHD is greater than that of the conventional hybrid tee discriminator [2]–[5]. However, the analysis of the ILHD made in [1] assumes an idealized situation where the practical circuit effects are assumed to be either absent or eliminated by proper arrangements.

This paper analyzes the influence of practical circuit implementations on the ILHD. Among the possible circuit effects, attention has been given to the presence of delay lines in different parts of the discriminator, amplitude perturbation of the injection-locked Gunn oscillator (ILGO), and the reflection resulting from a mismatch of the detector connected with the *E*-arm of the magic tee. Moreover, the structure of the ILHD as proposed in [1] is compared with the other possible structures, and the optimum structure is determined. Finally, a feedback mechanism has been proposed for the bandwidth extension of the ILHD so that the optimum ILHD can have more bandwidth than a simple injection-locked oscillator.

The possible applications for the ILHD in subsystems include the faithful recovery of signals in terrestrial and deep-space satellite communications and moving-target detection in a Doppler radar. It is well known that an injection-locked oscillator (ILO) possesses the property of FM- and external-noise squelching [6], [7]. Since the ILHD utilizes the technique of injection-locking, it is quite reasonable to expect that it will possess both the FM- and the external-noise-filtering property. This intrinsic noise-squelching property cannot be expected in a nontracking microwave discriminator [2], [5]. Making the crossover

Manuscript received January 3, 1986; revised June 17, 1986. This work was supported in part by the Ministry of Defence of the Government of India.

The author is with the Radionics Laboratory, Physics Department, Burdwan University, Burdwan 713 104, India.

IEEE Log Number 8611624.

frequency of the ILHD equal to the radar transmitter frequency, it can be used in the receiver of a Doppler radar system to estimate the radial velocity and to sense the direction of radial motion of the moving target. The effect of land clutter due to the echoes resulting from the fixed targets can be suppressed completely.

## II. ANALYSIS

A schematic block diagram of the ILHD that was discussed in [1] is shown in Fig. 1. The following analysis will be carried out assuming square-law operation of the diode detectors used in the implementation of the ILHD. We first consider the effect of the delay lines on the ILHD performance.

### A. Delay Line Preceding the Gunn Oscillator

Let us suppose that a waveguide line of length  $L$  is inserted between the Gunn oscillator (GO) and port 2 of the hybrid tee. Thus, the signal injected into the GO is delayed relative to the other component of the input signal moving towards the short. If this line corresponds to a phase delay of  $n\pi$  radians at the discriminator crossover frequency ( $\omega_c$ ), then  $L = n\pi c / (\omega_c^2 - \omega_{co}^2)^{1/2}$ , where  $n$  is a number corresponding to the line length  $L$ ,  $c$  is the vacuum velocity of light, and  $\omega_{co}$  is the cutoff frequency of the waveguide line used.

Let  $V_0 \cos \omega t$  be the input signal directed into the *H*-arm of the magic tee through the circulator. The signal splits at the junction into two identical components,  $V_0 / \sqrt{2} \cos \omega t$ . The component passing through the waveguide line undergoes a phase delay  $\varphi(\omega)$ , given by

$$\varphi(\omega) = n\pi \left( \frac{\omega^2 - \omega_{co}^2}{\omega_c^2 - \omega_{co}^2} \right)^{1/2}.$$

The synchronizing signal in the presence of the delay line is given by  $v_s(t) = V_0 / \sqrt{2} \cos(\omega t - \varphi(\omega))$ .

A number of investigations have been carried out on the injection-locking of microwave solid-state oscillators [8]–[11]. A series circuit equivalent representation [11] of the injection-synchronized Gunn oscillator is shown in Fig. 2, where  $R$ ,  $L$ , and  $C$  are, respectively, the resistance, inductance, and capacitance of the equivalent lumped circuit of the resonator, and  $R_L$  is the resistive load. The symbols  $r$  and  $c$  represent, respectively, the nonlinear resistance and the nonlinear capacitance of the oscillating Gunn diode. The potential drops across the elements  $r$  and

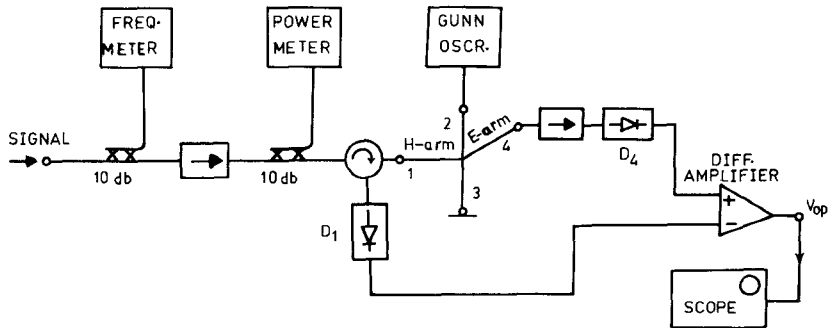


Fig. 1. Schematic circuit diagram of the injection-locked hybrid discriminator.

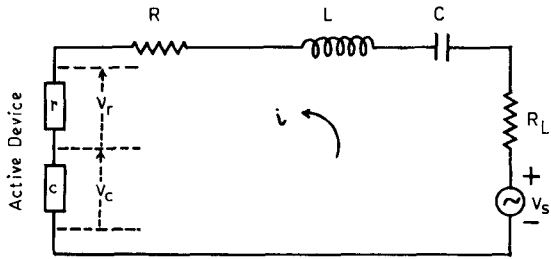


Fig. 2. Analytical equivalent circuit of the injection-locked Gunn oscillator.

$v_r(i)$  and  $v_c(i)$  are, respectively, denoted by  $v_r(i)$  and  $v_c(i)$ , which are nonlinear functions of the device current  $i$  and are assumed to be of the form [11]

$$v_r(i) = -\beta_1 i + \beta_2 i^2 + \beta_3 i^3 \quad (1)$$

and

$$v_c(i) = \alpha_1 q + \alpha_2 q^2 + \alpha_3 q^3 \quad (2)$$

where

$$i = \frac{dq}{dt} \quad (3)$$

and  $\alpha_n$  and  $\beta_n$  ( $n = 1, 2, 3$ ) are the constants characterizing the nonlinearity of the active device. Now, applying Kirchhoff's voltage law to the mesh shown in Fig. 2 and using (1)–(3), the equation of the GO in the presence of the injected signal can be written as [11]

$$\frac{d^2q}{dt^2} + \left[ -r_1 \frac{dq}{dt} + b_2 \left( \frac{dq}{dt} \right)^2 + b_3 \left( \frac{dq}{dt} \right)^3 + a_2 q^2 + a_3 q^3 \right] \frac{\omega_r}{Q_L} + \omega_r^2 (1 + C\alpha_1) q = \frac{\omega_r^2}{Q_L} q_s(t) \quad (4)$$

where

$$r_1 = \frac{\beta_1 - R - R_L}{R_L} \quad Q_L = \frac{\omega_r L}{R_L} \quad a_n = \frac{\alpha_n}{R_L}$$

$$b_n = \frac{\beta_n}{R_L} \quad (\text{for } n = 2, 3)$$

$$\omega_r = \frac{1}{\sqrt{LC}} \quad \text{and} \quad q_s(t) = Q_L C v_s(t).$$

Here,  $q$  is the instantaneous charge circulating through the device,  $Q_L$  is the  $Q$ -factor of the external circuit, and  $\omega_r$  is the resonant angular frequency of the cavity.

Assuming that the output of the injection-locked Gunn oscillator (ILGO) is of the form

$$q(t) = A(t) \sin(\omega t - \Psi(t))$$

and making use of the principle of harmonic balance [12], we obtain from (4) the following amplitude and phase equations:

$$\frac{da}{dt} = \frac{r_1 \omega_r}{2Q_L} \left[ 1 - \left( \frac{\omega}{\omega_0} \right)^2 a^2 \right] a + \frac{\omega_r^2}{2\omega Q_L} \sqrt{\frac{P_s}{P_0}} \cos(\Psi - \varphi) \quad (5)$$

$$\frac{d\Psi}{dt} = \frac{\omega_0}{2} \left( \frac{\omega}{\omega_0} - \frac{\omega_0}{\omega} \right) - \frac{3\omega_r^2 m a^2}{8Q_L \omega} - \frac{\omega_r^2}{2Q_L \omega a} \sqrt{\frac{P_s}{P_0}} \sin(\Psi - \varphi) \quad (6)$$

where  $a = A/A_0$  and  $m = a_3 A_0^2 / \omega_r$ ,  $A_0$  being the free-running amplitude of the GO.  $P_s$  and  $P_0$  are, respectively, the locking signal power and the output power of the GO. In the steady state of the ILGO,  $da/dt = 0$  and  $d\Psi/dt = 0$ . If  $V_{d1}$  and  $V_{d4}$  denote, respectively, the net signal appearing at the inputs of the detectors connected with the  $H$ - and  $E$ -arms of the magic tee, then in the presence of the delay line the output of the ILHD can be found as

$$V_{op} = \eta (|V_{d4}|^2 - |V_{d1}|^2) = \eta G V_0^2 \left[ \frac{a}{K_0} \left( \frac{\omega^2 - \omega_0^2}{2\omega_0} - \delta \right) \cdot \cos 2\varphi + r_1 a G \frac{\omega}{\omega_0} \left( \frac{\omega^2 a^2}{\omega_0^2} - 1 \right) \cdot \sin 2\varphi \right] \quad (7)$$

where  $\delta = 3m\omega_0 a^2 / 8Q_L$  is the locking asymmetry and  $\eta$  is the efficiency of the detectors assumed to be identical.  $G = (P_0/P_s)^{1/2}$  is the locking gain. Assuming low-level injection, the output power variation of the ILGO over the locking band is neglected so that we can put  $a \approx 1$ . Numerical solution of (7) is shown in Fig. 3. It is seen that the linearity and the frequency sensitivity of the discriminator response are affected adversely due to the ex-

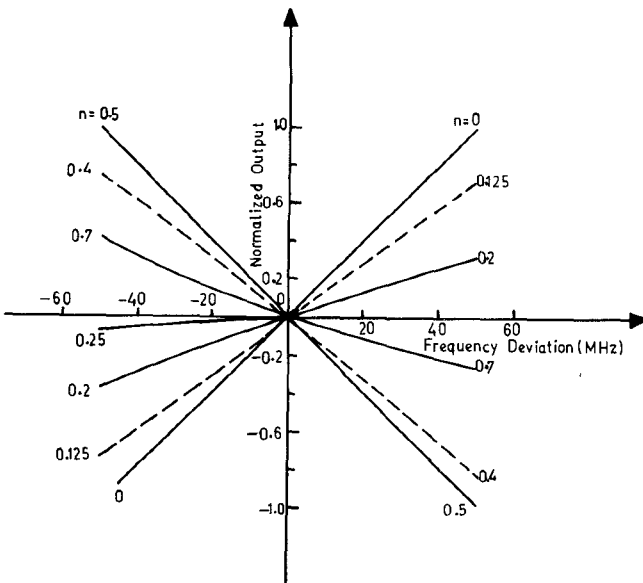


Fig. 3. ILHD response in the presence of a delay line preceding the Gunn oscillator,  $Q_L = 27.43$ ,  $P_0 = 48$  mW,  $P_s = 4$  mW. Locking range = 100 MHz; locking asymmetry factor  $m = -0.11$ ; Gunn oscillator frequency = 9.56 GHz; signal delay =  $n\pi$  radians; crossover frequency (with  $n = 0$ ) = 9.548 GHz.

istence of a delay line preceding the GO. The response changes its quadrants for line lengths corresponding to delays lying in the interval  $(2n-1)\pi/4 < \varphi(\omega_c) < (2n+1)\pi/4$  for  $n = 1, 3, 5, \dots$ . This indicates a phase change of the ILHD output by  $\pi$  radians. The operation of the discriminator practically collapses when the delay at the crossover frequency equals  $(2n+1)\pi/4$  radians for  $n = 0, 1, 2, \dots$ .

#### B. Delay Line Preceding the Metallic Short

In this section, we study the effect of a waveguide line placed at the end of port 3 of the magic tee, with the short now placed at the end of this waveguide line. This line introduces delay in the waves passing through port 3 of the magic tee. Proceeding in a manner similar to that in Section II-A, the output of the ILHD can be calculated as

$$V_{op} = \eta GV_0^2 \left[ \frac{a}{K_0} \left( \frac{\omega^2 - \omega_0^2}{2\omega_0} - \delta \right) \cos \varphi - r_1 a G \frac{\omega}{\omega_0} \left( \frac{\omega^2 a^2}{\omega_0^2} - 1 \right) \sin \varphi \right] \quad (8)$$

where

$$\varphi(\omega) = \pi + 2n\pi \left( \frac{\omega^2 - \omega_{co}^2}{\omega_c^2 - \omega_{co}^2} \right)^{1/2}$$

and the other symbols have their significances as stated earlier. Taking  $a \approx 1$ , a numerical solution of (8) is obtained and the frequency response of the normalized output of the ILHD,  $(V_{op}/\eta GV_0^2)$ , is shown in Fig. 4. The sensitivity and the linearity of response degrade due to the delay line. This degradation is least when the single-pass phase delay equals  $n\pi/2$  radians and is greatest when this

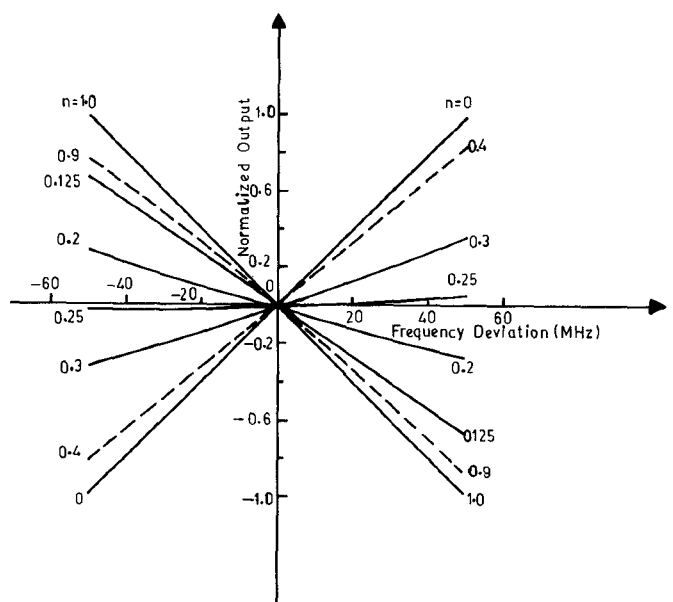


Fig. 4. ILHD response in the presence of a delay line preceding the short. Phase delay per pass =  $n\pi$  radians. Other parameters are identical with those in Fig. 3.

delay equals  $(2n+1)\pi/4$  radians for an integral  $n$  including zero. Reversal of the response occurs for lengths of the delay line corresponding to single-pass delay  $\varphi(\omega_c)$  lying in the interval  $(2n-1)\cdot\pi/4 < \varphi(\omega_c) < (2n+1)\cdot\pi/4$ , where  $n$  is an even integer.

#### C. Effect of Reflection from the E-Arm Detector

The detector connected with the *E*-arm of the magic tee may not, in general, be matched with the magic tee, and partial reflection of the detector input signal may occur due to this mismatch. The effect of such reflection on the ILHD performance can, however, be eliminated by connecting this detector to the magic tee through an isolator, as shown in Fig. 1. In this section, we are interested in investigating the effect of any reflection on the ILHD performance.

Let  $\rho$  denote the reflection coefficient, which is defined as the ratio of the amplitude of the reflected wave to that of the incident wave. Further,  $\rho$  is assumed to be real as well as small. The reflected wave splits at the hybrid junction into two components by equal power division which are identical except for a phase difference of  $\pi$  radians. The component emerging through port 3 of the hybrid tee gets reflected from the metallic short; it splits at the hybrid junction into two equiamplitude signals which pass through the *E*- and *H*-arms and appear at the inputs of the detectors connected with the respective arms. Since  $\rho$  is small, we neglect the effect of multiple reflections from the *E*-arm detector. In the presence of reflection, the phase equation of the ILGO reduces to

$$\frac{d\Psi}{dt} = \frac{\omega_0}{2} \left( \frac{\omega}{\omega_0} - \frac{\omega_0}{\omega} \right) - \frac{3\omega_r^2 m a^2}{8Q_L} - \frac{\omega_r K_0}{\omega} \left( 1 - \frac{\rho}{2} \right) \sin \Psi + \frac{\omega_r^2 \rho}{4Q_L \omega} \quad (9)$$

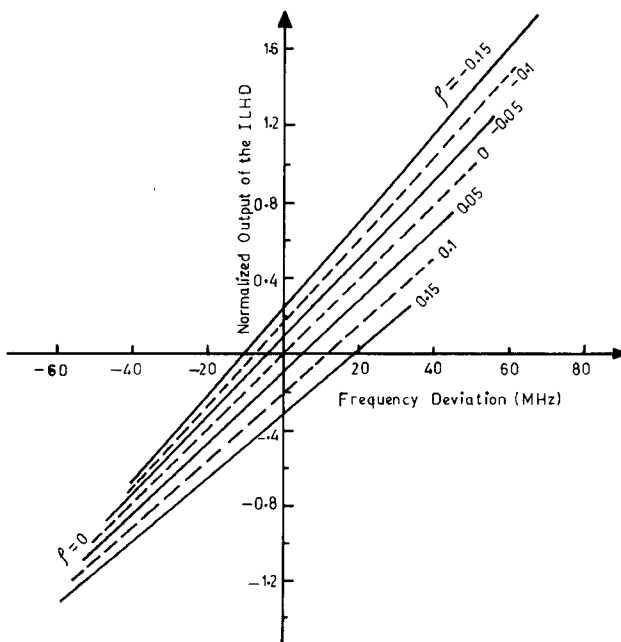


Fig. 5. ILHD response in the presence of reflection arising from a mismatch of the  $E$ -arm detector.  $\rho$  = reflection coefficient. Other parameters are the same as in Fig. 3.

where

$$K_0 = \frac{\omega_0}{2Q_L} \sqrt{\frac{P_s}{P_0}}.$$

In the steady state,  $d\Psi/dt = 0$ . From (9), it is seen that the locking range in the presence of reflection is  $2K_0(1 - \rho/2)$ . The last term in (9),  $\omega_r^2\rho/4Q_L\omega$ , modifies the locking asymmetry. The output of the ILHD can now be calculated as

$$V_{op} = \eta \frac{GV_0^2}{K_0} \frac{(2-3\rho)}{(2-\rho)} \left[ \frac{\omega^2 - \omega_0^2}{2\omega_0} - \delta \right] \quad (10a)$$

where

$$\delta = \frac{3\omega_0 m}{8Q_L} + \frac{2GK_0\rho}{2-3\rho} - \frac{GK_0\rho}{2} + \frac{K_0\rho}{G(2-3\rho)}. \quad (10b)$$

Here,  $\omega_c = \omega_0 + \delta$  gives the crossover frequency of the discriminator. Thus, the difference between the crossover frequency and the free-running Gunn oscillator frequency is not equal to the locking asymmetry ( $3\omega_0 m/8Q_L - K_0 G \rho/2$ ). The numerical solution of (10a) for different values of  $\rho$  is shown in Fig. 5. The most detrimental effect of reflection on the ILHD response is that the response becomes highly asymmetric on either side of the crossover frequency. This is because the center of the locking band is different from the crossover frequency. This response asymmetry increases with the magnitude of the reflection coefficient and leads to a reduction of the effective bandwidth of the ILHD. From Fig. 5, it is seen that when  $\rho$  is positive, the response is displaced toward the lower frequency side. The frequency band of the ILHD lying above the crossover frequency becomes less than that in the absence of reflection. For a negative reflection coefficient,

the response is affected oppositely and it gets displaced toward the higher frequency side. The crossover frequency increases for a positive reflection coefficient and decreases for a negative reflection coefficient from its value in the absence of reflection. This crossover frequency shift increases with the increase of reflection. However, linearity of the response is affected little due to the reflection from this detector.

#### D. Effect of Amplitude Perturbation of the ILGO

In deriving the frequency response equation of the ILHD [1], it is assumed that the output power of the ILGO remains constant at its free-running value over the entire locking band. This assumption is, however, valid for low-level injection. In general, the output power of the locked oscillator varies with the locking signal frequency. This amplitude perturbation increases with the power of the locking signal. Eliminating  $\Psi$  from the amplitude and phase equations, we get

$$A_1 a^6 - A_2 a^4 + A_3 a^2 - A_4 = 0 \quad (11)$$

where

$$\begin{aligned} A_1 &= \left( \frac{r_1 \omega^2}{2Q_L \omega_0} \right)^2 + \left( \frac{3\omega_0^2 m}{8Q_L \omega} \right)^2 \\ A_2 &= 2 \left( \frac{r_1 \omega}{2Q_L} \right)^2 + 2\Omega \left( \frac{3\omega_0^2 m}{8Q_L \omega} \right) \\ A_3 &= \left( \frac{r_1 \omega_0}{2Q_L} \right)^2 + \Omega^2 \\ A_4 &= \left( \frac{\omega_0 K_0}{\omega} \right)^2 \text{ and } \Omega = \frac{\omega_0}{2} \left( \frac{\omega}{\omega_0} - \frac{\omega_0}{\omega} \right). \end{aligned}$$

In the absence of reflection and signal delay, the output of the ILHD can be expressed as

$$V_{op} = \sqrt{2} \eta A_s V_0 \left[ \frac{\omega^2 - \omega_0^2}{2\omega_0} - \delta \right] \frac{a}{K_0} \quad (12)$$

where  $\delta = 3\omega_0 m a^2 / 8Q_L$  and  $A_s$  is the locked-oscillator amplitude. Thus, the discriminator output varies directly as the square root of the output power of the ILGO. This introduces nonlinearity into the response which, in turn, gives rise to harmonic distortion of the detected signal. This indicates that the locking band of the Gunn oscillator should be increased by employing a low- $Q$  resonator instead of increasing the locking signal power.

#### E. Comparison with Other Possible Implementations

In the implementation already discussed [1], the synchronizing signal is derived from the input signal by equal power division at the magic tee. We can, however, conceive of other implementations of the ILHD in which the synchronizing signal is not necessarily derived by the half power division of the input signal; rather, any desired fraction of the input signal can be used as the locking signal.

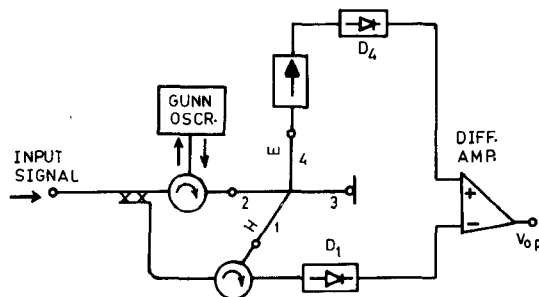


Fig. 6. Schematic circuit diagram of a possible implementation of the ILHD.

Let us first consider the implementation shown in Fig. 6. The input signal  $V_0 \cos \omega t$  is divided into two parts using a directional coupler. One part,  $xV_0 \cos \omega t$ , is directed into the  $H$ -arm of the hybrid tee through a coaxial cable or waveguide sections, while the other,  $(1-x)V_0 \cos \omega t$ , is injected into the Gunn oscillator. Proceeding in a similar way, we obtain the following expression for the output of this discriminator:

$$V_{op} = \sqrt{2} \eta A_s x V_0 \left[ \left( \frac{\omega^2 - \omega_0^2}{2\omega_0} - \delta \right) \frac{\cos \varphi}{K_0} + G \frac{\omega}{\omega_0} a^2 \left( 1 - \left( \frac{\omega a}{\omega_0} \right)^2 \right) \sin \varphi \right] \quad (13a)$$

where  $\varphi(\omega)$  is the phase delay of the signal entering the  $H$ -arm of the magic tee relative to that injected into the Gunn oscillator. The symbol  $\delta$  is the same as in (12).

Now, for the sake of comparison, we take  $\varphi(\omega_c) = 2n\pi$ , where  $n$  is the integer corresponding to the smallest possible length of the coaxial cable or the waveguide line directing the signal into the  $H$ -arm of the magic tee. Again, assuming  $2K_0 \ll \omega_c$ , we can neglect the variation of  $\varphi(\omega)$  over the discriminator band. Equation (13a) now reduces to

$$V_{op} = \sqrt{2} \eta A_s \frac{x V_0}{K_0} \left( \frac{\omega^2 - \omega_0^2}{2\omega_0} - \delta \right). \quad (13b)$$

The figure of merit of the ILHD, which is defined as the frequency sensitivity-bandwidth product, is given by

$$F_{I1} = \frac{dV_{op}}{d\omega} \Big|_{\omega = \omega_c} \cdot 2K_0 = 2\sqrt{2} \eta A_s x V_0. \quad (13c)$$

Under low-level injection, the locked-oscillator amplitude  $A_s$  is nearly constant over the discriminator band. Then, for a given input signal,  $F_{I1}$  is maximum when  $x = 1$ , that is, when the entire signal is directed into the  $H$ -arm of the magic tee. But, as  $x$  increases, the discriminator bandwidth decreases and the bandwidth practically vanishes when  $x \rightarrow 1$ . So, the optimum implementation should be one in which the locking signal is obtained by half power division of the input signal. This leads to the conclusion that the structure shown in Fig. 1 is the optimum structure of the ILHD.

Another possible circuit configuration of the ILHD is shown in Fig. 7. Here, the input signal  $V_0 \cos \omega t$  is divided

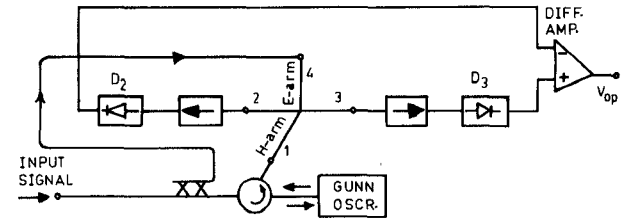


Fig. 7. Schematic circuit diagram for a second possible implementation of the ILHD.

into two components,  $xV_0 \cos \omega t$  and  $(1-x)V_0 \cos \omega t$ , by using a directional coupler. The Gunn oscillator is locked to the signal  $(1-x)V_0 \cos \omega t$  and its output,  $A \sin(\omega t - \Psi)$ , splits into two identical components at the hybrid junction, which appear at the inputs of the detectors, as usual. The other part of the input signal,  $xV_0 \cos(\omega t - \varphi)$ , generates a pair of waves having equal amplitude but opposite phase. The members of this pair propagate oppositely and arrive at the detector inputs. The output of this ILHD is given by

$$V_{op} = 2\eta A_s V_0 x \sin(\Psi - \varphi) \quad (14a)$$

where  $\varphi$  is the relative phase delay produced by the coaxial cable. The bandwidth-sensitivity product can be calculated as

$$F_{I2} = 4\eta V_0 A_s x. \quad (14b)$$

Reasoning as before, we put  $\varphi = 2n\pi$ , where  $n$  is an integer, for comparing this implementation with that described in [1]. For a given input signal power and under low-level injection, the only adjustable parameter is  $x$ . If  $x$  is reduced, the figure of merit of the system degrades. On the other hand, an increase in  $x$  leads to a decrease in locking power and hence to a reduction in the bandwidth of the discriminator. This also leads to the conclusion that the locking signal should be derived by equal power division of the input signal for the optimum design of the ILHD.

Apart from this aspect of merit, the implementations shown in Figs. 6 and 7 possess design complexity and are likely to be affected by the signal delay produced by the coaxial cable. It follows from the discussions of Sections II-A and II-B that the signal delay affects the frequency sensitivity and the linearity of response adversely. This performance degradation becomes more pronounced, especially for long coaxial cables when the phase delay  $\varphi(\omega)$  varies significantly over the bandwidth of the discriminator.

#### F. Bandwidth Extension

Since the bandwidth of the ILHD is equal to the locking band of the Gunn oscillator, the discriminator bandwidth can be increased by extending the lock band of the ILGO. It is well known [11] that the locking range of a Gunn oscillator can be extended considerably by controlling the bias of the oscillator. Hence, to improve the bandwidth of the ILHD, the bias control technique can be utilized. For this, the ILHD output is amplified and then added with

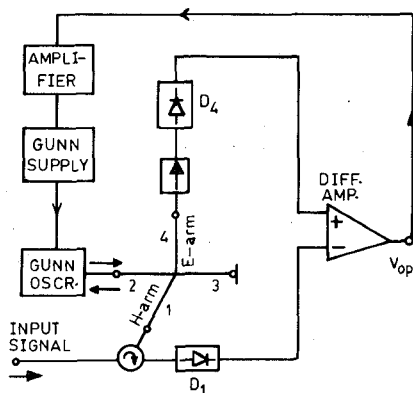


Fig. 8. Schematic circuit diagram for the extended-band ILHD.

the Gunn supply voltage. The total output of the Gunn supply source is now the sum of a constant dc voltage and a control voltage which is proportional to the discriminator output. A schematic diagram of the proposed extended-band ILHD is shown in Fig. 8. To explain how this extension of the locking band occurs, we should remember that the output power and the oscillation frequency of the Gunn device are functions of the Gunn bias voltage. Typical plots of the bias-voltage dependence of the power and frequency of the 9.636-GHz Gunn oscillator can be found in [11], from which it is apparent that both the power and the frequency of the Gunn oscillator vary almost linearly with the bias voltage around this frequency of operation. Considering the operation of the bias-compensated ILGO, we see that in upper-side locking (i.e., when  $\omega > \omega_0$ ), the output is positive and its magnitude increases with the locking signal frequency. This increased output of the ILHD increases the Gunn bias through the feedback and results in a proportional increase of the power and the frequency of the Gunn oscillator. Increase of the Gunn oscillator frequency leads to a reduction of the effective detuning of the locking signal from the Gunn oscillator. Obviously, the upper-side locking band will increase. The increased output of the ILHD, however, tends to reduce the pull of the locking signal on the Gunn oscillator; this, in effect, reduces partly the enhancement of the locking band produced by the feedback voltage. In lower-side locking, the negative output voltage of the discriminator reduces the Gunn bias, resulting in a decrease in the power and frequency of the oscillator. In this case, reductions of both the power and the frequency of the Gunn oscillator favor the enhancement of the locking band.

The lock band of an oscillator can be increased by lowering the circuit  $Q$  or by increasing the locking power. But, for a given  $Q$  and a given locking power, this bias-compensation technique always gives an additional benefit in increasing the locking range.

### III. CONCLUSIONS

The performance degradation of the ILHD in relation to its frequency sensitivity, linearity, and bandwidth in the presence of delay lines placed at different parts of the

circuit has been studied analytically. Practical circuit effects such as the amplitude variation of the locked oscillator over the discriminator bandwidth and the reflection originating from a detector mismatch can lead to a deterioration of the ILHD response. The optimum structure for the ILHD is determined and the possibility of its bandwidth extension through Gunn-bias compensation is established.

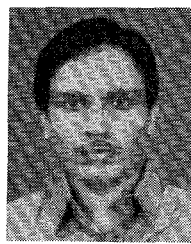
### ACKNOWLEDGMENT

The author is grateful to Prof. B. N. Biswas, Department of Physics, Burdwan University.

### REFERENCES

- [1] T. P. Chattopadhyay, "An injection-locked hybrid microwave discriminator," *Proc. IEEE*, vol. 74, pp. 746-748, May 1986.
- [2] P. Z. Peebles and A. H. Green, "A microwave discriminator at 35 GHz," *Proc. IEEE*, vol. 68, pp. 286-288, Feb. 1980.
- [3] H. S. Shaik and P. Z. Peebles, "Practical effects in the response of a microwave discriminator," in *Proc. of Southeast Conf.* (Huntsville, AL), 1981, pp. 487-490.
- [4] H. S. Shaik, "Analysis of a practical microwave discriminator," M.S.E.E. thesis, University of Tennessee, Knoxville, TN, Jan. 1981.
- [5] T. P. Chattopadhyay and B. N. Biswas, "Improved X-band FM discriminator," *IEEE Trans. Microwave Theory Tech.*, vol. MTT-34, pp. 442-446, Apr. 1986.
- [6] T. Sugiura and S. Sugimoto, "FM noise reduction of Gunn-effect oscillators by injection locking," *Proc. IEEE*, vol. 57, pp. 77-78, Jan. 1969.
- [7] S. K. Ray and K. Pramanik, "Recovery of signals by a unilaterally coupled oscillator," in *Proc. Seminar on Time and Frequency*, National Physical Laboratory (India), Nov. 1976, pp. 188-203.
- [8] K. Daikoku and Y. Mizushima, "Properties of injection locking in the non-linear oscillator," *Int. J. Electron.*, vol. 31, pp. 279-292, Mar. 1971.
- [9] K. Kurokawa, "Injection locking of microwave solid-state oscillator," *Proc. IEEE*, vol. 61, pp. 1386-1410, Oct. 1973.
- [10] M. Nakajima and J. Ikenoue, "Locking phenomena in microwave oscillator circuits," *Int. J. Electron.*, vol. 44, pp. 465-472, 1978.
- [11] B. N. Biswas, S. K. Ray, K. Pramanik, M. Sadhu, and D. Bandyopadhyay, "Hold-in characteristics of an extended range Gunn oscillator system," *IEEE Trans. Microwave Theory Tech.*, vol. MTT-31, pp. 271-276, Mar. 1983.
- [12] C. Hayashi, *Nonlinear Oscillations in Physical Systems*. New York: McGraw-Hill, 1964, pp. 28-32.

✉



**Taraprasad Chattopadhyay** was born at Katwa, West Bengal, India, on September 6, 1957. He received the B.Sc. degree (with honors) in physics and the M.Sc. degree in physics, with specialization in electronics, from the University of Burdwan in 1977 and 1979, respectively.

He joined the Radionics Laboratory at Burdwan University as a junior research fellow in February 1982. In the same year, he was selected by the Public Service Commission, West Bengal, for the post of Lecturer in Physics in the West Bengal Educational Service, a post which he took up in April 1983. At present, Mr. Chattopadhyay is a Lecturer in the Department of Physics, Krishnagar Government College, West Bengal. Since April 1983, he has conducted part-time research work in the Radionics Laboratory at Burdwan University.